Egypt. J. Chem. **Vol. 67**, No. 12 pp. 537 - 555 (2024)

Egyptian Journal of Chemistry

http://ejchem.journals.ekb.eg/

New Modified Benzimidazole Derivatives Carried on Different Sugars and Nanocrystalline Cellulose: Anticancer and Antioxidant Activity Estimation

Tamer I. M. Ragab[a]*, Hadeer Saadoun[b], Mohammed T. Abdel Aal[b], Ibrahim F. Nassar[c], Samah A. El-Newary[d]

[a]*Chemistry of Natural and Microbial Products Department, Pharmaceutical Industries and Drug Research Institute, National Research Centre, Dokki 12622, Cairo, Egypt*
[b]*Chemistry Department, Faculty of Science, Menoufia University, Shebin El-Kom, 32511 Egypt*
[c]*Faculty of Specific Education, Ain Shams University, Abassia, Cairo, 3251Egypt*
[d]*Medicinal and aromatic plant research Department, Pharmaceutical Industries and Drug Research Institute, National Research Centre, Dokki 12622, Cairo, Egypt*

Abstract

Some heterocyclic compounds of 2-methyl thio-1H-benzimidazol were newly synthesized carried on different mono, disaccharides and nanocrystalline cellulose. The extracted cellulose was obtained from cotton stalk agro-wastes. Nanocrystalline cellulose (NCC) was prepared and characterized by (FTIR, SEM and HRTEM). The synthesized benzimidazol sugars and NCC were evaluated for their potential anticancer and antioxidant activities. All the added sugars; mannose, xylose, and maltose significantly increased 2-methyl thio-1H-benzimidazol anticancer activity against breast carcinoma cells (MCF-7), and colon carcinoma cells (HCT-116). Mannose substitution (compound 7) recorded the highest activity against both cancer cell lines (IC_{50}, 29.90 ± 0.92 and 50.45 ± 3.06 µg/ml, respectively), compared to benzimidazol compound (122.86 ± 3.17 and 218.47 ± 5.93 µg/ml, respectively). Unfortunately, the acetylated sugars and nanocrystalline cellulose derivatives compounds have less activity than their original compounds depending on decreasing the free hydroxyl groups. On contrast, NCC benzimidazol derivative showed anticancer activity less than all substituted sugars benzimidazol derivatives (IC_{50}, 144.04 ± 6.07 and 405.85 ± 16.38 µg/ml, respectively), meanwhile, the acetylated NCC benzimidazol increased as anticancer activity (IC_{50}, 98.12± 4.31 and 206.18 ± 6.59 µg/ml, respectively). Also, the antioxidant activity of the new synthesized compounds was performed showing good activity.

Keywords*:* Benzimidazole; Nano-crystalline cellulose; Anticancer activity; Antioxidant activity.

1. Introduction

Breast cancer is a disease caused by abnormal breast cells that multiply and form tumors. If left untreated, tumors have the capacity to spread throughout the body and become fatal. The first places where breast cancer cells multiply are the milk-producing lobules and the milk ducts in the breast. The first type, referred to as "in situ," is not life-threatening and can be detected early. Cancer cells have the ability to infiltrate nearby breast tissue. This causes tumors that grow or develop lumps. The process by which invasive tumors spread to nearby lymph nodes or other organs is known as metastasis. Metastasis has the potential to be deadly or fatal. The patient, the type of cancer, and the amount of its dissemination all influence the course of treatment. Treatment options include radiation therapy, medication, and surgery. Breast cancer is a global disease that can strike women at any stage after puberty, while it becomes more common as people age [1].

*Corresponding author e-mail: tamerragab2006@gmail.com.;(Tamer I. M. Ragab).
EJCHEM use only: Received date 24 September 2024; revised date 27 October 2024; accepted date 30 October 2024
DOI: 10.21608/ejchem.2024.322046.10509
©2024 National Information and Documentation Center (NIDOC)

Global estimations show stark differences in the incidence of breast cancer based on human development. For example, in nations with a very high Human Development Index (HDI), 1 in 12 women may receive a breast cancer diagnosis during their lifetime, and 1 in 71 will pass away from the disease. In comparison, 1 in 48 women will pass away from breast cancer in nations with a low HDI, even though only 1 in 27 women will receive a diagnosis of the disease during their lifetime. Combinations of symptoms, particularly in more advanced cases, can indicate breast cancer. These include a) thickening or lumping of the breast; b) frequently without pain; c) changes in the size, shape and appearance; d) redness, dimpling and pitting in the skin; e) changes in the nipple or the skin surrounding it; and f) bloody fluid from nipple [1].

Colorectal cancer is kind of cancer that affects the colon or rectum. It is among the most prevalent forms of cancer in the globe. It can result in death or serious injury. As people age, their chance of colorectal cancer were rises. The majority of instances impact those over 50. Constipation, diarrhea, blood in the stool, exhaustion, low iron levels and inexplicable weight loss are typical symptoms. Many people with the condition won't show any signs when it's first developing. Limiting alcohol use, eating a nutritious diet, quitting smoking, and maintaining physical activity can all help lower the risk of colorectal cancer. Screenings on a regular basis are essential to early detection.

When it comes to cancer-related deaths worldwide, colon cancer comes in second. More than 1.9 million new cases of colorectal cancer and 930,000 deaths from the disease were predicted to occur globally in 2020. Regional variations in the incidence and death rates were noteworthy. The highest incidence rate was found in Europe, Australia, and New Zealand, while the highest fatality rate was found in Eastern Europe. By 2040, it is anticipated that the yearly burden of colorectal cancer would increase to 3.2 million new cases and 1.6 million deaths. In high-income nations, colorectal cancer incidence rates have been declining, partly due to successful screening initiatives. Depending on the stage upon diagnosis, colorectal cancer has varying prognoses. The survival rate of early-stage malignancies is higher than that of advanced-stage tumors. Improving survival rates and quality of life requires prompt diagnosis, suitable treatment, and routine follow-up care [2].

Due to its biological activity and practical utility, benimidazole and its derivatives have drawn a lot of interest [3-5]. They can be found in a wide range of pharmaceuticals and naturally occurring goods [6, 7]. According to Chohan et al. (2008) and Sanja et al. (2002), several of these substances exhibit anti-bacterial, anti-viral, anti-fungal, anti-inflammatory, anti-hypertensive, arteriosclerosis, anti-cancer, and anti-HIV properties [3, 8].

Cellulose has emerged as one of the most effective polymeric nanoparticles utilized for delivery systems due to its unmatched biocompatibility and biodegradability [9]. According to Naomi et al. (2020), Cellulose is a linear homopolymer composed of 1,4-1inked D-anhydroglucopyranosyl units. It is mostly present in fibrils in its natural crystalline form [10]. Particularly, the plant-based cellulose has important qualities since it is safe and stable due to the hardness of hydrogen bonding, which requires strong acids and alkalis or aprotic solvents to dissolve. This sorts it useful for pharmaceutical activities [11]. Agricultural wastes and byproducts are a rich source of cellulose, even though they usually pose a threat to the environment [12]. To address this, efforts to transform unwanted agro-based processing litter into goods with a marketable potential have been ongoing [13, 14].

This study was focused on synthesized benzimidazol mono-, di-, and polysaccharides compounds. Extraction cellulose from cotton stalks agro-waste and then nano-crystalline cellulose preparation. Sugars benzimidazol and nanocrystalline cellulose derivatives were evaluated as anticancer and antioxidant.

2. Materials and methods

2.1. Mammalian cell lines, drugs and chemicals

The American Type Culture Collection (ATCC, Rockville, MD) provided the MCF-7 human breast cancer cells and the HCT-116 colon cancer cell line. Dimethyl sulfoxide, crystal violet (0.5% (w/v) crystal violet and 50% methanol then made up to volume with ddH_2O and filtered through a Whatmann No.1) and trypan blue dye were purchased from Sigma (St. Louis, Mo., USA). Fetal Bovine serum, DMEM, RPMI-1640, HEPES buffer solution, L-glutamine, gentamycin and 0.25% Trypsin-EDTA were purchased from Lonza. L-ascorbic acid (vitamin C), Trolox, potassium ferricyanide, Trichloro acetic acid (TCA), ferric chloride ($FeCl_3$), 1,1-diphenyl-2-picryl-hydrazyl (DPPH), 2,2-azino-bis(3-ethylbenz-thiazoline-6-sulfonic acid (ABTS), peroxidase, hydrogen peroxide. Analytical-grade chemicals and reagents were acquired from regional scientific distributors in Egypt for use in this study.

2.2. Analytical Instrumentals

Melting points are uncorrected and were calculated using a Kofler block device. ^1H and ^{13}C-NMR spectra were measured on a Varian Gemini spectrometer (300 MHz) using DMSO-d_6 as a solvent

and TMS (δ) as the internal standard. Mass spectra were obtained using a CC 2010 Shimadzu Gas chromatography instrument mass spectrometer (70 eV). The progress of the reactions was monitored by TLC using aluminum silica gel plates 60 F245. The anticancer activity of the synthesized compounds was carried out at the Regional Center for Mycology & Biotechnology, Al-Azhar University, Cairo, Egypt.

2.3. Experimental

2.3.1. 2-{[(1-(2-Chloroethyl)-1H-benzo[d]imidazol-2-yl)thio]methyl}thiazole (2).

To a solution of 2-{[(1H-benzo[d]imidazol-2-yl)thio]methyl}thiazole 1 (2.47 g, 10 mmol) in dry acetone (10 mL), potassium carbonate (1.38 g, 10 mmol) was added and the solution was stirred at room temperature for 1 h. Dichloroethane (0.74 mL, 10 mmol) was added at room temperature and was continued stirring for 24 h. The resulting solution was filtered off, washed with dry acetone, then let the filtrate diminished at room temperature until the formed residue was appeared, dried and recrystallized. The formed residue was crystallized from acetone to give 2 as brown crystals; yield 66%; m.p.198-200°C. IR cm^{-1} νmax: 2950, 2875 cm^{-1} (ν CH alkane), 1635, 1447 cm^{-1} (C=C Ar), 875 cm^{-1} (C-Cl). ^{1}H-NMR (DMSO-d6, δ ppm) =3.98 (t, 2H, CH_2), 4.32 (s, 2H, CH_2), 4.68 (t, 2H, CH_2), 7.08-7.42 (m, 4H, Ar-H) ppm. ^{13}C-NMR (DMSO-d6, 125 MHz): δ 35.49, 44.23, 60.00 (3 CH_2), 110.23-167.89 (Ar-C) ppm. EI-MS: m/z ($C_{13}H_{12}ClN_3S_2$) calc d = 309 [M^+].

2.3.2. 2-{{{ [1-(2-azidoethyl)-1H-benzo[d]imidazol-2-yl]thio}methyl}}thiazole (3).

A solution of 2 (3.09 g, 10 mmol) in (10 mL) DMF, sodium azide (0.65 g, 10 mmol) and ammonium chloride (0.53 g, 10 mmol) were added and refluxed for 8 h. The resulting solution was concentrated then cooled to room temperature then poured onto ice and acidified with HCl. The obtained precipitate was filtered off, dried, and recrystallized from EtOH to give 3 as brown crystals; yield 63%, m.p. 198-200°C. IR cm^{-1} νmax: 2960, 2925, 2854 cm^{-1} (ν CH alkane), 2164 cm^{-1} (ν N3), 1632, 1464 cm^{-1} (C=C Ar). ^{1}H-NMR (DMSO-d_6, δ ppm) = 2.19 (t, 2H, CH_2), 3.97 (t, 2H, CH_2), 4.39 (s, 2H, CH_2), 7.08-7.62 (m, 4H, Ar-H) ppm. ^{13}C-NMR (DMSO-d_6, 125 MHz): δ 32.00, 41.31, 68.79 (3CH_2), 110.03-164.49 (Ar-C) ppm.

2.3.3. 5-methyl-1-{{2-{2-[(thiazol-2-ylmethyl)thio]-1H-benzo[d]imidazol-1-yl}ethyl}}-1H-1,2,3-triazole-4-carboxylic acid (4).

A solution of sodium ethoxide (20 ml), 3 (3.16 g, 10 mmol), ethyl acetoacetate (1.27 mL, 10 mmol) were added and refluxed for 18 h. The resulting solution was concentrated then cooled to room temperature then poured onto ice. The obtained precipitate was filtered off, dried, and recrystallized from EtOH to give 4 as brown crystals; yield 61%, m.p. 198-200°C. IR cm^{-1} νmax: 3419 cm^{-1} (ν OH), 2925, 2854 cm^{-1} (ν CH alkane), 2210 cm^{-1} (ν triazole ring), 1658 cm^{-1} (ν C=O), 1626 cm^{-1} (C=N), 1545, 1433 cm^{-1} (C=C Ar). ^{1}H-NMR (DMSO-d_6, δ ppm) = 2.46 (s, 1H, CH_3), 4.37 (s, 2H, CH_2), 4.67 (t, 2H, CH_2), 4.82 (t, 1H, CH_2), 9.91 (br. S, 1H, OH), 7.07-7.60 (m, 4H, Ar-H) ppm. ^{13}C-NMR (DMSO-d_6, 125 MHz): δ 9.21(CH_3), 36.16, 48.82, 49.28 (3 CH_2), 117.58-154.97 (Ar-C), 173.68 (C=O) ppm.

2.3.4. Ethyl5-methyl-1-{{2-{2-[(thiazol-2-ylmethyl)thio]-1H-benzo[d]imidazol-1-yl}ethyl}}-1H-1,2,3-triazole-4-carboxylate (5).

H_2SO_4 (10 mL) was added to a solution of 4 (4.00 g, 10 mmol) in ethanol (20 mL) and refluxed for 4 hours. After that, the mixture was allowed to cool at ambient temperature. After filtering, drying, and recrystallizing the resulting precipitate from EtOH, 5 brown crystals were produced; yield was 67%, m.p. 198–200°C. IR cm^{-1} νmax: 3088 cm^{-1} (ν CH alkene), 2926 cm^{-1} (ν CH alkane), 1647 cm^{-1} (ν C=O), 1572 cm^{-1} (ν C=N), 1524, 1410 cm^{-1} (C=C Ar). ^{1}H-NMR (DMSO-d_6, δ ppm) = 1.24 (t, 3H, CH_3), 2.46 (s, 1H, CH_3), 4.15 (q, 2H, CH_2), 4.35 (s, 2H, CH_2), 4.53 (t, 2H, CH_2), 4.70 (t, 1H, CH_2), 6.99-7.59 (m, 4H, Ar-H) ppm. ^{13}C-NMR (DMSO-d_6, 125 MHz): δ 9.22 (CH_3), 14.21 (CH_3), 36.16, 48.82, 49.28, 63.08 (4CH_2), 117.58-154.97 (Ar-C), 180.88 (C=O) ppm.

2.3.5. 5-Methyl-1-{{2-{2-[(thiazol-2-ylmethyl)thio]-1H-benzo[d]imidazol-1-yl}ethyl}}-1H-1,2,3-triazole-4-carbohydrazide (6).

To a solution of 5 (4.28 g, 10 mmol) in absolute ethanol (10 ml), hydrazine hydrate (2.4 mL, 50 mmol) was added and refluxed for 8 h and at 25°C.. The obtained precipitate was filtered off, dried, and recrystallized from EtOH to give 6 as brown crystals; yield 65%, m.p. 197-201°C. IR cm^{-1} ν max: 3444, 3422, 3074 cm^{-1} (ν NH_2, NH), 2956, 2924, 2853 cm^{-1} (ν CH alkane), 1622 cm^{-1} (ν C=O), 1561 (ν C=N), 1512, 1413 cm^{-1} (C=C Ar). ^{1}H-NMR (DMSO-d_6, δ ppm) = 2.31 (s, 1H, CH_3), 4.32 (s, 2H, CH_2), 4.38 (t, 4H, 2CH_2), 4.41 (br.s, 2H, NH_2 exchangeable), 7.22-7.30 (m, 4H, Ar-H), 7.51 (br.s, 1H, 1 NH exchangeable) ppm. ^{13}C-NMR (DMSO-d_6, 125 MHz): δ 7.79 (CH_3), 39.92, 40.08, 40.26 (3CH_2), 110.03-153.00 (Ar-12 C), 164.49 (C=O) ppm.

2.3.6. (E)-5-Methyl-N'-(2,3,4,5,6-pentahydroxyhexylidene)-1-{{2-{2-[(thiazol-2-ylmethyl)thio]-1H-benzo[d]imidazol-1-yl}ethyl}}-1H-1,2,3-triazole-4-carbohydrazide (7).

The hydrazide derivatives 6 (3.86 g, 10 mmol) were added to a well-stirred combination of D-(+)-mannose (1.80 g, 10 mmol) in water (1 ml), glacial acetic acid (0.2 ml) in ethanol (10 ml). After eight hours of reflux heating, the mixture was concentrated and allowed to cool. The precipitate that had formed was removed by filtering, cleaned with ethanol and water, dried, and then recrystallized from ethanol to produce 7 brown crystals with a yield of 62% at 199–202°C. IR cm^{-1} νmax: 3441 cm^{-1} (ν OH), 3553 cm^{-1} (ν NH), 2924, 2855 cm^{-1} (ν CH alkane), 1622 cm^{-1} (ν C=O, C=N), 1622, 1455 cm^{-1} (C=C Ar). ^{1}H-NMR (DMSO-d_6, δ ppm) =1.79 (s, 3H, CH_3), 2.28, 2.38, 2.46 (t, 3H, 3CH), 2.60 (q, 1H, CH), 2.69 (d, 2H, CH_2), 2.85, 3.08, 3.32 (br.s, 4H, 4 OH), 4.19 (s, 2H, CH_2), 4.65 (t, 4H, $2CH_2$), 7.22-7.92 (m, 7H, Ar-H), 9.77 (br.s, 1H, 1 NH exchangeable) ppm. ^{13}C-NMR (DMSO-d_6, 100 MHz) δ= 9.09 (1C, CH_3), 39.95 (1C, CH_2), 40.29, 40.45 (2C, $2CH_2$), 51.65 (1C, CH_2), 60.14, 70.46, 76.06 (3C, 3CH), 109.48-156.63 (13C, C-Ar), 170.87 (C=O) ppm.

2.3.7. (E)-5-Methyl-N'-(2,3,4,5-tetrahydroxypentylidene)-1-{{2-{2-[(thiazol-2-ylmethyl)thio]-1H-benzo[d]imidazol-1-yl}ethyl}}-1H-1,2,3-triazole-4-carbohydrazide (8).

Glacial acetic acid (0.2 ml) in ethanol (10 ml) was added to a well-stirred mixture of D-(+)-xylose (1.80 g, 10 mmol) in water (1 ml) and the hydrazide derivatives 6 (3.86 g, 10 mmol). After eight hours of reflux heating, the mixture was concentrated and allowed to cool. After filtering off the precipitate, the mixture was cleaned with ethanol and water, dried, and then the ethanol was recrystallized to yield 8 brown crystals (yield 69%, m.p. 199–203°C. IR cm^{-1} νmax: 3548 cm^{-1} (ν NH), 3447 cm^{-1} (ν OH), 2924, 2855 cm^{-1} (ν CH alkane), 1623 cm^{-1} (ν C=O, C=N), 1517, 1454 cm^{-1} (C=C Ar). ^{1}H-NMR (DMSO-d_6, δ ppm) =1.85 (s, 3H, CH_3), 2.38, 2.46 (t, 2H, 2CH), 2.60 (q, 1H, CH), 2.69 (d, 2H, CH_2), 2.85, 3.08, 3.32 (br.s, 4H, 4 OH), 4.19 (s, 2H, CH_2), 4.63 (t, 4H, $2CH_2$), 7.22-7.92 (m, 7H, Ar-H), 8.37 (br.s, 1H, 1 NH exchangeable). ^{13}C-NMR (DMSO-d_6, 100 MHz) δ= 8.03 (1C, CH_3), 39.95 (1C, CH_2), 40.29, 40.45 (2C, $2CH_2$), 51.65 (1C, CH_2), 60.14, 70.46, 91.89 (3C, 3CH), 104.63-156.63 (13C, C-Ar), 170.87 (C=O) ppm.

2.3.8. N'-3,4-Dihydroxy-6-(hydroxymethyl)-5-3,4,5-trihydroxy-6-(hydroxymethyl)tetrahydro-2H-pyran-2-yl)oxy)tetrahydro-2H-pyran-2-yl)methylene)-5-methyl-1-(2-(2-((thiazol-2-ylmethyl)thio)-1H-benzo[d]imidazol-1-yl)ethyl)-1H-1,2,3-triazole-4-carbohydrazide (9).

Glacial acetic acid (0.2 ml) in ethanol (10 ml) was added to a well-stirred mixture of D-(+)-maltose (3.42 g, 10 mmol) in water (1 ml) and the hydrazide derivatives 8 (3.86 g, 10 mmol). After eight hours of reflux heating, the mixture was concentrated and allowed to cool. The precipitate that had formed was removed by filtering, cleaned with ethanol and water, dried, and then recrystallized from ethanol to produce 9 brown crystals with a yield of 64% at 195–198°C. IR cm^{-1} νmax: 3434 cm^{-1} (ν OH, NH), 2923, 2856 cm^{-1} (ν CH alkane), 1636 cm^{-1} (ν C=O, C=N), 1509, 1460 cm^{-1} (C=C Ar). ^{1}H-NMR (DMSO-d_6, δ ppm) =1.82 (s, 3H, CH_3), 3.33-3.45 (t, 9H, 9 CH), 3.90 (d, 4H, $2CH_2$), 4.49-4.87 (br.s, 7H, 7OH), 4.19 (s, 2H, CH_2), 4.39 (t, 4H, $2CH_2$), 6.09 (s, 1H, CH), 7.06-7.98 (m, 7H, Ar-H), 8.53 (br.s, 1H, 1 NH exchangeable). ^{13}C-NMR (DMSO-d_6, 100 MHz) δ= 9.21 (1C, CH_3), 40.71(1C, CH_2), 47.27, 48.12 (2C, $2CH_2$), 61.71 (2C, $2CH_2$-OH), 68.71, 76.70, 77.22, 85.00, 90.43 (10C, 10CH), 111.01-160.01 (13C, C-Ar), 168.03 (C=O) ppm.

2.3.9. (1S)-1-(3-Acetyl-5-(5-methyl-1-(2-(2-((thiazol-2-ylmethyl)thio)-1H-benzo[d]imidazol-1-yl)ethyl)-1H-1,2,3-triazol-4-yl)-2,3-dihydro-1,3,4-oxadiazol-2-yl)butane-1,2,3,4-tetrayl tetraacetate (10)

A 5.48 g, 10 mmol solution of sugar hydrazones 7 was heated under reflux for 1.5 hours in 15 ml of acetic anhydride. The final mixture was added to crush ice, and the precipitate product was filtered out, cleaned with a sodium hydrogen carbonate solution and water, and allowed to dry. After being recrystallized from ethanol, 10 brown crystals with a yield of 65% and a melting point of 198–200°C were obtained. IR cm^{-1} νmax: 2926, 2856 cm^{-1} (ν CH alkane), 1743 cm^{-1} (ν C=O), 1580 cm^{-1} (ν C=N), 1580, 1424 cm^{-1} (C=C Ar). ^{1}H-NMR (DMSO-d_6, δ ppm) =1.82 (s, 3H, CH_3), 2.38, 2.47, 2.63, 2.75, 2.90 (s, 15H, $5CH_3$), 4.12, 4.21(t, 4H, $2CH_2$), 5.16 (d, 2H, CH_2), 5.98 (s, 2H, CH_2), 6.53, 6.63 (d, 2H, 2CH), 6.87 (q, 1H, CH), 7.14 (d, 1H, CH), 7.24-8.63 (m, 6H, Ar-H). ^{13}C-NMR (DMSO-d_6, 100 MHz) δ= 9.09 (1C, CH_3), 20.96, 21.87, 22.99 (5C, $5CH_3$), 39.90, 40.08, 40.24 (3C, $3CH_2$), 63.74, 63.90, 64.08 (3C, 3CH), 64.24 (1C, CH_2), 78.92 (1C, CH), 116.23-160.82 (13C, C-Ar), 170.17, 170.53, (5C, Ac) ppm.

2.3.10. (1S)-1-{{{{3-Acetyl-5-{{{5-methyl-1-{{2-{2-[(thiazol-2-ylmethyl)thio]-1H-benzo[d]imidazol-1-yl}ethyl}}-1H-1,2,3-triazol-4-yl}}}-2,3-dihydro-1,3,4-oxadiazol-2-yl}}}}propane-1,2,3-triyl triacetate (11)

For 1.5 hours, a solution of sugar hydrazones 8 (5.18 g, 10 mmol) in 15 ml of acetic

anhydride was cooked under reflux. The final mixture was added to crush ice, and the product was filtered out, cleaned with a sodium hydrogen carbonate solution and water, and allowed to dry. After being recrystallized from ethanol, 11 brown crystals with a yield of 69% and a melting point of 192–194°C were obtained. IR cm^{-1} νmax: 2926, 2855 cm^{-1} (ν CH alkane), 1743 cm^{-1} (ν C=O), 1626 cm^{-1} (ν C=N), 1626, 1457 cm^{-1} (C=C Ar). ^{1}H-NMR (DMSO-d_6, δ ppm) =1.82 (s, 3H, CH_3), 2.38, 2.47, 2.63, 2.75 (s, 12H, $4CH_3$), 4.12, 4.21 (t, 4H, $2CH_2$), 5.16 (d, 2H, CH_2), 5.98 (s, 2H, CH_2), 6.53 (d, 1H, 1CH), 6.87 (q, 1H, CH), 7.14 (d, 1H, CH), 7.24-8.63 (m, 6H, Ar-H). ^{13}C-NMR (DMSO-d_6, 100 MHz) δ= 9.09 (1C, CH_3), 20.96, 21.87, 22.99 (4C, $4CH_3$), 39.90, 40.08, 40.24 (3C, $3CH_2$), 63.90, 64.08 (2C, 2CH), 64.24 (1C, CH_2), 78.92 (1C, CH), 116.23-160.82 (13C, C-Ar), 170.17- 176.12 (4C, Ac) ppm.

2.3.11. Acetoxymethyl-6-((4,5-diacetoxy-6-((S)-3-acetoxy-5-(5-methyl-1-(2-(2-((thiazol-2-ylmethyl)thio)-1H-benzo[d]imidazol-1-yl)ethyl)-1H-1,2,3-triazol-4-yl)-2,3-dihydro-1,3,4-oxadiazol-2-yl)-2-(acetoxymethyl)tetrahydro-2H-pyran-3-yl)oxy)tetrahydro-2H-pyran-3,4,5-triyl triacetate (12)

For one and a half hours, a solution of 9 (7.22 g, 10 mmol) in 15 ml of acetic anhydride was cooked under reflux. The final mixture was added to crush ice, and the product was filtered out, cleaned with a sodium hydrogen carbonate solution and water, and allowed to dry. After being recrystallized from ethanol, 12 brown crystals with a yield of 65% and a melting point of 198–201°C were obtained. IR cm^{-1} ν max: 2926, 2857 m^{-1} (ν CH alkane), 1767 (ν C=O acetyl), 1711 cm^{-1} (ν C=O amide), 1649 cm^{-1} (ν C=N), 1649, 1518 cm^{-1} (C=C Ar). ^{1}H-NMR (DMSO-d_6, δ ppm) = (2.02, 2.06, 2.08, 2.32, 2.66, 2.72, 2.88, 2.94 (s, 24H, $8OCH_3$), 2.78 (s, 3H, CH_3), 3.16 (s, 10H, $5CH_2$), 5.75 (m, 10H, 10CH cyclohexanone), 7.36 (m, 6H, Ar-H). ^{13}C-NMR (DMSO-d_6, 100 MHz) δ= 14.14 (1C, CH_3), 20.82, 21.10, 30.74 (8C, $8OCH_3$), 48.65, 54.94 (3C, $3CH_2$), 59.83 (2C, $2CH_2$-OAc), 78.65, 80.05 (9C, CH cyclohexanone), 125.37-137.42 (13C, C-Ar), 172.12 (8C, 8Ac) ppm.

2.3.12. 5-3,4-Dihydroxy-6-(hydroxymethyl)-5-metheyliumyltetrahydro-2H-pyran-2-yl-oxy-3,4-dihydroxy-6-{{{{{(Z)-{{{{2-{{{5-methyl-1-{{2-{2-[(thiazol-2-ylmethyl) thio]-1H-benzo[d]imidazol-1-yl} ethyl}}-1H-1,2,3-triazol-4-yl}}}hydrazono}}}}methyl}}}}}tetrahydro-2H-pyran-2-yl-oxymethylium (13)

Glacial acetic acid (0.2 mL) in EtOH (10 mL) was added to a stirred mixture of nano cellulose (3.86 g, 10 mmol) in water (1 mL) that had been dissolved in 6 (3.86 g, 10 mmol) in DMF (10 mL). After eight hours of reflux heating, the mixture was concentrated and allowed to cool. After filtering off the precipitate, the filtrate was allowed to cool. After filtering out the precipitate, 13 black powders (yield 54%, m.p. 300°C) were obtained. IR cm^{-1} ν max: 3428 cm^{-1} (ν OH, NH), 3003 (ν CH aromatic), 2925, 2855, 2727cm^{-1} (ν CH aliphatic), 1630 cm^{-1} (ν C=O, C=N), 1498 cm^{-1} (C=C Ar). ^{1}H-NMR (DMSO-d_6, δ ppm) =1.99 (s, 1H, CH_3), 3.55 (m, 9H, 5OH, $2CH_2$), 7.22-7.51 (m, 4H, Ar-H), 8.57 (br.s, 1H, 1 NH exchangeable) ppm.

2.3.13. 4,5-Diacetoxy-2-(acetoxymethyl)-6-4,5-diacetoxy-6-(metheyliumyloxy)-2-((Z)-(2-(5-methyl-1-(2-(2-((thiazol-2-ylmethyl)thio)-1H-benzo[d]imidazol-1-yl)ethyl)-1H-1,2,3-triazol-4-yl)hydrazono)methyl)tetrahydro-2H-pyran-3-yl)oxy)tetrahydro-2H-pyran-3-yl)methylium (14)

13 (7.22 g, 10 mmol) in 15 ml of acetic anhydride was brought to a boil under reflux for a duration of 1.5 hours. The final mixture was added to crush ice, and the separated product was filtered out, cleaned with a sodium hydrogen carbonate solution and water, and allowed to dry. After being recrystallized from ethanol, 14 black powder with a yield of 66% and a melting point of 200–202°C were obtained. IR cm^{-1} ν max: 3444 cm^{-1} (ν NH), 2920, 2859 cm^{-1} (ν CH alkane), 1735 cm^{-1} (ν C=O), 1636 cm^{-1} (ν C=O, C=N), 1428 cm^{-1} (C=C Ar). ^{1}H-NMR (DMSO-d_6, δ ppm) =2.12 (s, 3H, CH_3), 2.59-3.10 (m, 12H, $5CH_3$), 4.17-4.79 (m, 8H, $4CH_2$), 6.88 (d, 1H, 1CH), 6.99 (q, 1H, CH), 7.08 (d, 1H, CH), 7.20-8.18 (m, 6H, Ar-H), 8.87 (br.s, 1H, 1NH exchangeable) ppm.

2.3.14. Cellulose Extraction and Purification

Using an alkaline potassium hydroxide 2% (1:20 w/v) treatment at 90°C for three hours, followed by filtering, crude cellulose was recovered from cotton stalk waste. After drying the raw cellulose residue at 70ºC, sodium hypochlorite (1:1 w/w) was used to bleach it. Following a thorough wash with distilled water till neutralization, the bleached cellulose was fully dried at 70°C. After bleaching the cellulose, it was treated with 17.5% alkaline potassium hydroxide and filtered to extract the α-cellulose [15].

2.3.15. Nano-crystalline cellulose preparation and characterization

Following a two-hour period of continuous and intense mechanical shaking in an acid medium (2N H_2SO_4, 1:10 w/v), the obtained α-cellulose was hydrolyzed under reflux to yield nano-crystalline cellulose (NCC). After being fully cleaned with distilled water, the hydrolyzed NCC was dried [16].

SEM and TEM studies were used to identify the samples' crystalline size and shape.

2.3.16. Dissolving Nano-crystalline cellulose

NCC (5 g) was added in water (10 mL) and stirred with heating less than 40 °C for 1 h, and then MeOH (10 ml) was added with stirring for 1 h. Then the formed cellulose was added to DMAC and stirred well overnight. The precipitate was filtered off and dried. Wet cellulose was refluxed with DMAC (50 mL) at 150°C for 10 min. Then at 100 °C for 20 min. 4g of LiCl was added to the reaction mixture and refluxed at 50 °C for 15 min to give binary solution. Binary solution was stirred with heating at 25°C for 22h then at 4°C for 2-6 days to give completely dissolution. IR (KBr) cm^{-1} vmax: 3442 cm^{-1} (ν OH), 2934 cm^{-1} (ν CH aliphatic).

2.3.17. FT-IR spectroscopy

By using infrared analysis, the materials were characterized and identified. The NCC, NCC imidazole, and NCC imidazole acetylated powder were used to directly capture IR spectra, which were then recorded onto a detector prism using a Bruker Vectra 22 FT-IR Spectrometer fitted with a Dura Sample IR II™ detector. Every spectrum was captured within the wave number range of 4000-400 cm^{-1}, with a spectral resolution of 4 cm^{-1}.

2.3.18. Scanning Electron Microscopy (SEM) analysis

With an accelerating voltage of 10 kV, a scanning electron microscope (JEOL 5410) was used to analyze the surface morphology of the sample. A Hitachi coating unit IB-2 coater was used to gold coat NCC at high voltages of 1.2 kV and 50 mA, along with high vacuum and 0.1 Torr [17].

2.3.19. High Resolution Transmission Electron Microscopy (HRTEM) analysis

NCC particle size and shape were determined with a JEOL JEM 1011 (Japan) transmission electron microscope. 400 µL of nanoparticle solution was deposited on carbon-coated copper grids (400 meshes) and dried at 30°C before image capture [18].

2.4. Antioxidant properties estimation

The antioxidant abilities of the new modified benzimidazole derivatives were estimated using several methods. Five concentrations from each compound were prepared in methanol as 1000, 500, 250, 125, and 63 µg/ml. The antioxidant abilities of the compounds were calculated by comparing them with L-ascorbic acid and Trolox that was prepared with the same procedure. All tested were performed spectrophotometrically using (Jasco, serial No. C317961148, Japan) in the National Research Centre, Egypt.

2.4.1. Free radical scavenging capacity

DPPH radical scavenging: was assessed as mentioned by [19]. The DPPH solution (0.1 mM) in methanol was added to 3 ml of 1 ml of each concentration was shaken then was stand for 50min at 25-27°C. The produced color was recorded using spectrophotometer at 517 nm. The radical scavenging ability was performed by the formula;

$$(\%) = 100 - [(A_0\text{-}A_1)/A_0) \times 100]$$

Where A_0 (control absorbance) and A_1 (tested sample absorbance).

$ABTS^+$ radical scavenging: The whole antioxidant capacity of the samples was determined by applying the techniques [20, 21]. To replicate a bluish green complex, a mixture of 4.4 units/ml of peroxidase (0.2 ml), 50 µM of H_2O_2 (0.2 ml), 100 µM of ABTS (0.2 ml), and one mL of distilled water was held at 25°C in the dark for one hour. Following the addition of the drug or standard (1 ml), the absorbance was measured at 734 nm. The formula executed the ability to scavenge radicals;

$$\% = [1\text{-} (A_{sample} /A_{control})] \times 100$$

Where A_{sample} is sample absorbance or standards whereas $A_{control}$ is control absorbance.

2.4.2. Total reduction capability

Reduction capability of samples and standard materials; Vitamin C and Trolox, was estimated by the method of [22]. Each concentration was mixed vigorously with 2.5 ml phosphate buffer (200 mM, pH 6.6) and 2.5 ml potassium cyanoferrate (1%). The mixture was incubated for 20 min at 50 °C and then 2.5 ml of TCA portion (10%) was added to the mixture and then was centrifuged at 1000g for 10 min. 2.50 ml of solution upper layer was mixed with 2.5 ml distilled water and 0.5 ml of $FeCl_3$ (0.1%). The absorbance was measured at 700 nm spectrophotometrically.

2.5. Cell line Propagation

Dulbecco's modified Eagle's medium (DMEM) supplemented with 10% heat-inactivated fetal bovine serum, 1% L-glutamine, HEPES buffer, and 50 µg/ml of gentamycin was used to cultivate the cells. Each cell was subcultured three times a week and maintained at 37ºC in 5% CO_2 humidified air [23].

2.6. Cytotoxicity evaluation using viability assay

To conduct a cytotoxicity experiment, 100 µl of growth media was used to seed 1×104 cells per

well in 96-well plates. After 24 hours of seeding, fresh medium with variable quantities of the test sample was introduced. Confluent cell monolayers were transferred into 96-well flat-bottomed microtiter plates (Falcon, NJ, USA) using a multichannel pipette and successive two-fold dilutions of the chemical component being tested were then added. The micro titer plates were maintained at 37ºC in a humidified incubator with 5% CO_2 for duration of twenty-four hours. Three wells were used for each concentration of the test material. Control cells were grown either without the test substance or with DMSO. The tiny amount of DMSO (maximum 0.1%) in the wells was found to have no effect on the experiment. The viable cell yield was measured using a colorimetric method after a 24-hour incubation period at 37°C. In summary, after the incubation period, the media were aspirated, and the 1% crystal violet solution was added to each well for at least 30 minutes. The dishes were carefully cleansed with tap water to remove any last traces of discoloration once it was removed. The plates were gently shaken on a microplate reader (TECAN, Inc.) to measure the absorbance of the layers using a test wavelength of 490 nm after adding 30% glacial acetic acid to each well and thoroughly mixing them. All values were modified to take into consideration the background absorbance present in wells without additional stain. The treated samples were compared to the cell control in the absence of the chemicals that were studied. Each experiment was conducted three times. The cytotoxic impact of each examined chemical on cells was estimated. Using a microplate reader (SunRise, TECAN, Inc., USA), the optical density was measured in order to determine the number of viable cells. The percentage of viability was computed as [(ODt/ODc)] x100%, where ODt represents the mean optical density of wells treated with the tested sample and ODc represents the mean optical density of untreated cells. The survival curve of each tumor cell line following treatment with the designated substance is obtained by plotting the relationship between remaining cells and drug concentration. Using Graphpad Prism software, the 50% inhibitory concentration (IC_{50}), or the concentration needed to produce harmful effects in 50% of intact cells, was calculated using graphic plots of the dose response curve for each conc (San Diego, CA. USA) [24].

2.7. Statistical Analysis

The least significant test was used for multiple comparisons after repeated measures one-way analysis of variance (ANOVA) was used for statistical analysis. When the effects are $p < 0.05$, they are deemed significant. The mean ± standard error is used to express the results.

3. Results

3.1. Chemistry

In this investigation, thiazole derivative **2** was synthesized by reaction of 2-{[(1H-benzo[d]imidazol-2-yl)thio]methyl}thiazole **1** [25] and dichloroethane in dry acetone and in the presence of a basic medium in 66% yield. Azidoethyl thiazole derivative **3** was synthesized by reaction of **2** with sodium azide in DMF in presence of basic medium in 63% yield. Triazole carboxylic acid derivative **4** was synthesized by reaction of **3** with ethyl acetoacetate in absolute ethanol in presence of basic medium in 61% yield. Triazole carboxylate derivative **5** was synthesized by reaction of **4** with sulfuric acid in absolute ethanol in 67% yield. Hydrazide derivative **6** was synthesized by reaction of **5** with hydrazine hydrate in absolute ethanol in 65% yield (Scheme 1).

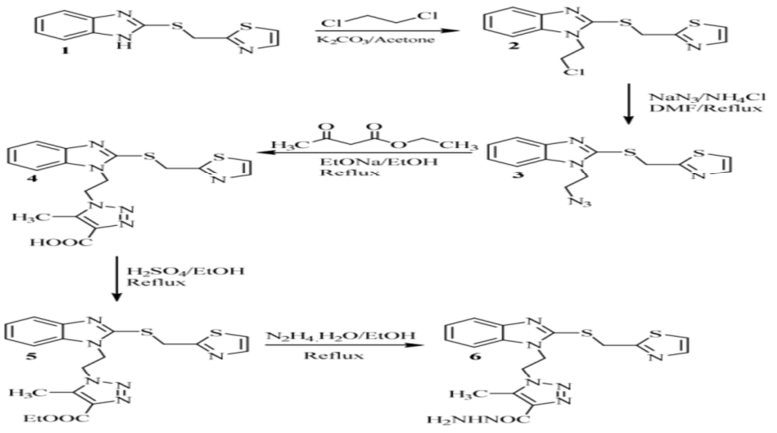

Scheme 1; Synthesis of compounds 2-6

Sugar hydrazone **7**, **8**, **9** was obtained in 62, 69, 64 % yield after refluxing of **6** with D-(+)-mannose, D-(+)-xylose, D-(+)-maltose in absolute ethanol and in the presence of a catalytic amount of glacial acetic acid (Scheme 2).

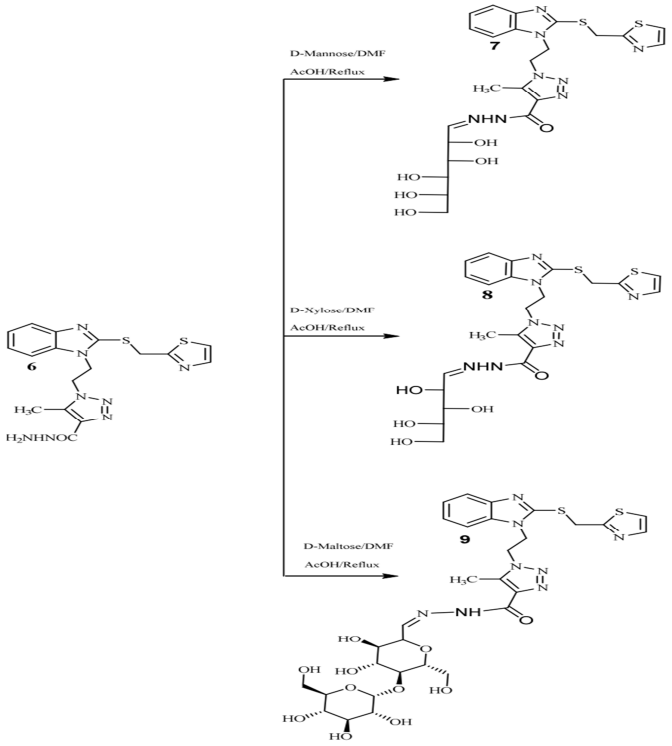

Scheme 2

Acetylation of **7** was performed by refluxing with acetic anhydride to afford tetrayl tetraacetate derivative **10** in 65% yield (Scheme 3).

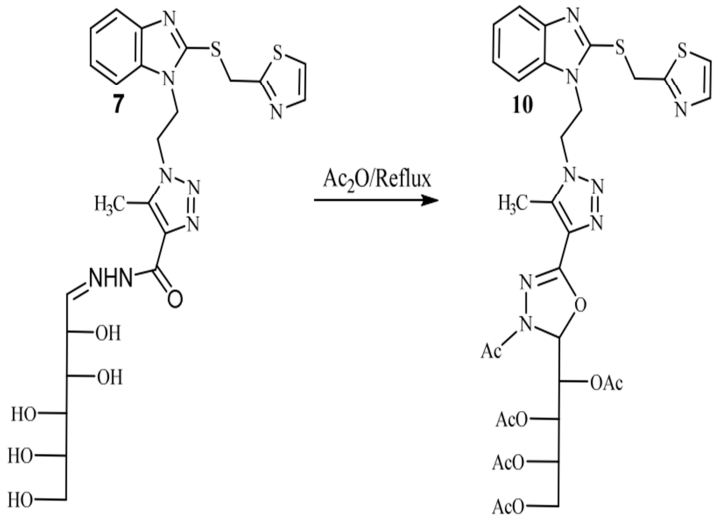

Scheme 3

Acetylation of **8** was performed by refluxing with acetic anhydride to afford triyl triacetate derivative **11** in 69% yield (Scheme 4).

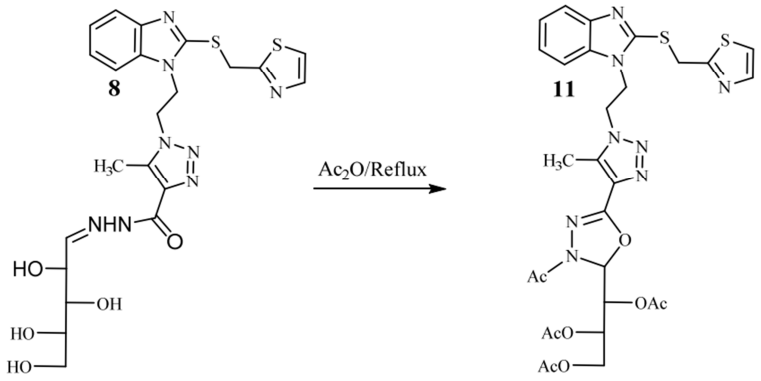

Scheme 4

Acetylation of **9** was performed by refluxing with acetic anhydride to afford pyran triyl triacetate derivative **12** in 65% yield (Scheme 5).

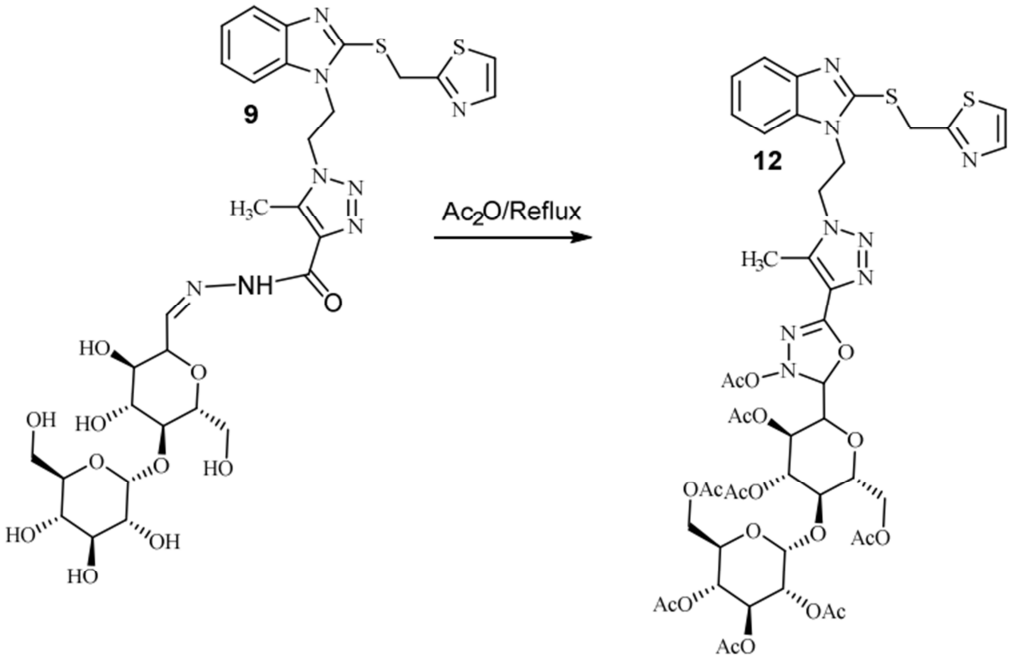

Scheme 5

Compound **13** was obtained in 54 % yield after refluxing of **6** with nanocellulose in DMF and in the presence of a catalytic amount of glacial acetic acid. Acetylation of **13** was performed by refluxing with acetic anhydride to afford **14** in 66% yield (Scheme 6).

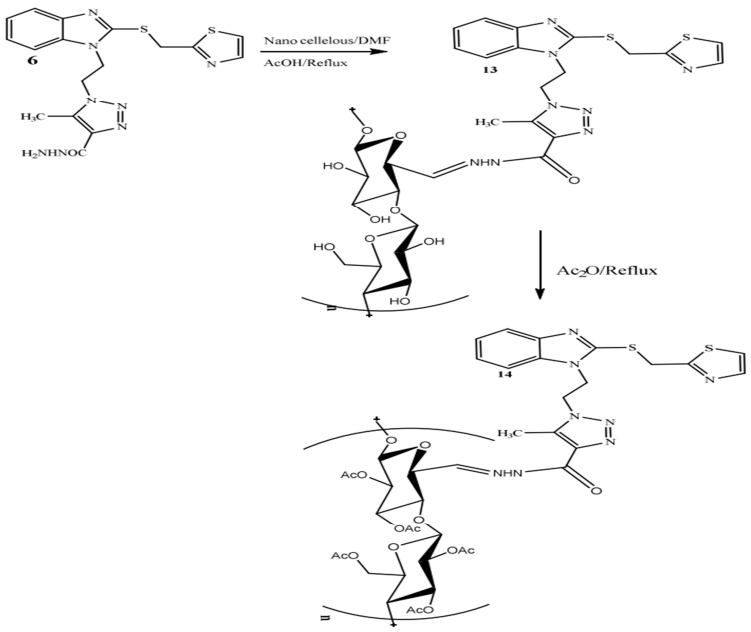

Scheme 6

3.2. **NCC preparation and characterization**

Cellulose 51.92%, hemicellulose 19.15%, and lignin 28.93% made up the cotton stalk agro-waste. This shown that cotton stalk might be a reliable cellulose supply. The majority of the hemicellulose and lignin were effectively removed by the treatments, leaving high (81.23%) cellulose content. NCC cotton stalk was produced after acid hydrolysis and yielded 32%.

3.3. FTIR analysis

FTIR spectroscopy is used to identify, scan, evaluate, and observe chemical characteristics of nanocellulose, nanocellulose imidazole derivatives and nanocellulose imidazole acetylated as shown in (Fig. 1). The stretching vibration of OH groups caused the absorption broadband of 3300–3550 cm^{-1}. The peak at 1560 cm^{-1} was attributed to the anti-symmetric C-O-C stretching bridge, whereas the peak at 2900–2950 cm^{-1} was related to the C-H stretching and vibration of the CH_2 cellulose group. The C-O-C stretching vibrations of the cellulose, also known as ring stretching, were linked to the absorption bands at 1040–1100 cm^{-1}. The -glycosidic bond between glucose units and the characteristic -CH rocking vibrations of the cellulose backbone is proposed to be located in the band at 870 cm^{-1}.

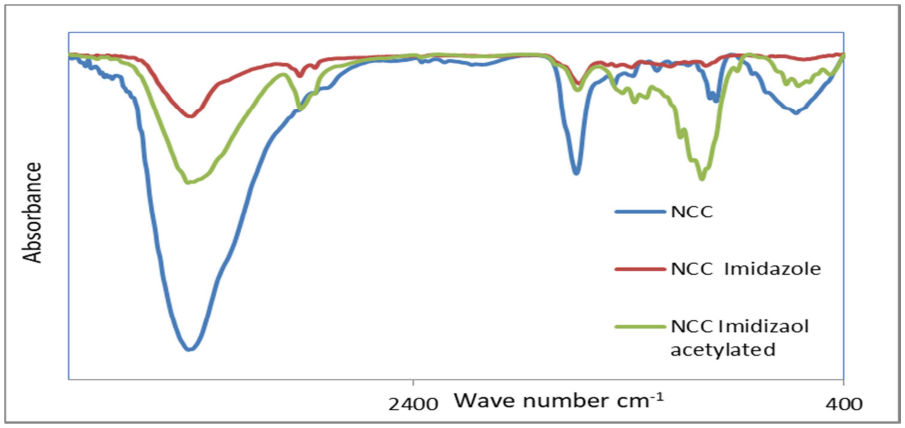

Figure 1: Fourier transforms infrared spectroscopy (FTIR) of NCC, NCC benzimidizole and NCC benzimidizole acetylated.

3.4. SEM and HRTEM analysis

Using scanning electron microscopy, the surface morphology of cotton stalk nanocellulose was investigated (Fig. 2a). Cotton stalk nanocrystalline cellulose particles have a rod-like structure. As seen in (Fig. 2b), the prepared NCC was measured for size and form using the HRTEM technique. Rod-like forms were the defining characteristics of NCC. The particle sizes of NCC ranged from 20 to 90 nm. NCC is in the critical nano-size range, measuring less than 100 nm.

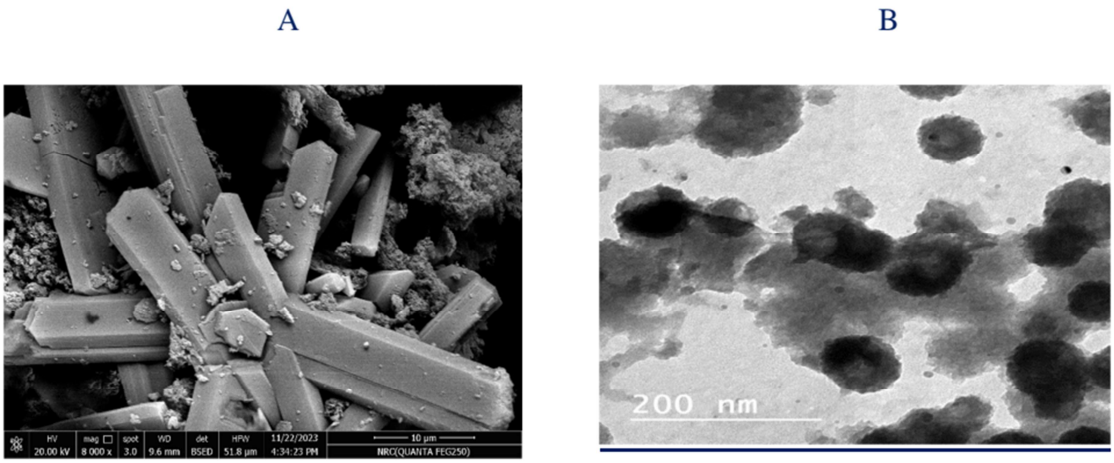

Figure 2: (A) Scanning electron microscopy (SEM) pictures of NCC cotton stalk and (B) High-resolution transmission electron microscopy (HRTEM).

3.5. Assessment of *in vitro* antioxidants properties

Antioxidant characters of synthetic compounds from Compound 6 to Compound **14** are presented in Table (1). Antioxidant characters of compounds are estimated by three methods including free radicals scavenging (DPPH and $ABTS^{+}$) and reducing power activities. To evaluate the Antioxidant characters, their activities are compared with two reference materials: L-ascorbic acid and Trolox. The antioxidant characters were presented as IC_{50} value. IC_{50} is the concentration of antioxidant material that can inhibit 50% of the free radicals' molecules in the reaction medium. Low IC_{50} means high antioxidant ability.

3.5.1. Free radicals scavenging (DPPH and $ABTS^{+}$)

Compound 6 neutralized the radical DPPH· and transferred it to the non-radical stable form ($p < 0.05$) by donating hydrogen atom. The concentration 0.590 µg/ml of the Compound **6** neutralized 50% of DPPH· radical form molecules (IC_{50}) concerning L- ascorbic acid and Trolox; 27.290 and 17.079 µg/ml. Compounds **7** and **8**; adding monosaccharide such as mannose (hexoses monosaccharide) or xylose (pentoses monosaccharide) to compound **6** significantly increased its ability to scavenge DPPH, where IC_{50} reduced from 0.59 µg/ml in compound **2** to 0.543 and 0.41 µg/ml with about 8% and 30.5% increase in the activity, respectively. On contrast in compound **9** adding maltose (disaccharide) to compound **6** dramatically decreased DPPH scavenging activity as IC_{50} significantly increased to 122.99 µg/ml, compared to that of the compound **6** (0.59 µg/ml).

Compounds **10**, **11** and **12** are acetylation of compounds **7**, **8** and **9** significantly changed their ability to scavenge DPPH. In the case of compound **10** and **12** (mannose and maltose), acetylation augmented their DPPH scavenging ability more than the original compound **7** and **9** by about 69.43% and 130.96%, respectively. IC_{50} of the origin compound **7**, **9** were elevated from 0.411 and 122.99 µg/ml to 0.166 and 0.932 µg/ml by acetylation. Meanwhile, compound **11** showed the opposite trend. Acetylation compound **8** to produce compound **11** significantly reduced its ability to scavenge DPPH radicals that evident by the increase in IC_{50} from 0.411 µg/ ml in original compound (**8**) to 1.752 in acetylated compound (**11**) with 326.28%.

In compound **13**, adding cellulose to compound 6 significantly minimized its ability to scavenge DPPH radicals according to IC_{50} value. IC_{50} of compound **13** was higher than that of compound **6** by about 700 times. Acetylation compound **13** produced compound **14**. Compounds 14 recorded DPPH scavenging activity higher than that of original compound (**13**). IC_{50} of compound **14** was lower than that of compound **13** by about 46.65%.

Finally, all compounds have DPPH radicals scavenging effect better than both reference materials. Compared to compound **6**, adding sugars molecules did not elevate its ability to scavenging

DPPH, except compound **7**, **8** and **10** that elevated DPPH scavenging activity. Compound **10** recorded the highest DPPH activity as the lowest LC_{50} (0.166 µg/ml). Compound **10** IC_{50} was lower than IC_{50} of L-ascorbic acid by about 164.4 times, Trolox (103 times), and compound **6** (3.55 times).

Table 1: Antioxidant activities of heterocyclic derivatives of 2-methylthio-1*H*-benzimidazol and reference materials; L-Ascorbic acid and Trolox

	Free radicals scavenging ability		Reducing power
Sample	DPPH	$ABTS^+$	Fe^{3+} ion Reductive
	IC_{50} (µg/ml)	IC_{50} (µg/ml)	IC_{50} (µg/ml)
Compound 6	0.590 ± 0.01^{ab}	0.8250 ± 0.01^{ab}	> 1000
Compound 7	0.543 ± 0.01^{ab}	0.736 ± 0.01^{ab}	> 1000
Compound 8	**0.411 ± 0.01^{ab}**	**0.557 ± 0.01^{ab}**	> 1000
Compound 9	122.985 ± 0.56^{ab}	169.77 ± 0.56^{ab}	**120.45 ± 0.55^{a}**
Compound 10	**0.166 ± 0.01^{ab}**	**0.225 ± 0.01^{ab}**	366.10 ± 0.45^{ab}
Compound 11	1.752 ± 0.05^{ab}	2.577 ± 0.05^{ab}	377.10 ± 0.11^{ab}
Compound 12	0.932 ± 0.03^{ab}	1.265 ± 0.03^{ab}	230.93 ± 0.50^{ab}
Compound 13	4.87 ± 0.01^{ab}	6.603 ± 0.01^{ab}	> 1000
Compound 14	3.321 ± 0.01^{ab}	4.553 ± 0.01^{ab}	> 1000
L- Ascorbic acid	27.290 ± 0.03	61.955 ± 0.03	78.16 ± 0.40
Trolox	17.079 ± 0.03	12.620 ± 0.03	120.62 ± 0.16

DPPH, (free radical). Data presented as mean ± SE. Independent T-test was used for data analysis (n=3, $p<0.05$). Data are followed with small letters; a means significant difference with L-Ascorbic acid, b means significant difference with Trolox.

$ABTS^+$ showed the same trend as DPPH. Compound **6** (the starter compound) recorded $ABTS^+$ capacity more than that recorded by reference materials; L- ascorbic acid or Trolox. According to IC_{50} values, compound **6** was a potent $ABTS^+$ scavenger agent better than L-ascorbic acid or Trolox; 0.825, 61.955, and 12.62 µg/ml, respectively). IC_{50} of compound **6** lower than L-ascorbic acid or Trolox by about (75 and 15 times, respectively).

Compared to compound **6**, adding sugars on compounds; **7**, **8**, and **9** changed their $ABTS^+$ scavenging activity between increase and decrease. Adding both mannose and xylose significantly increased $ABTS^+$ scavenging activity, meanwhile adding maltose significantly decreased it. IC_{50} of compounds **7** and **8** significantly decreased by about 10.88 and 32.48% that that of compound **6**, meanwhile IC_{50} of compound **9** significantly increased by about 205 times.

Acetylation compounds: **7**, **8**, and **9** that produced compounds **10**, **11**, and **12**, respectively significantly changed $ABTS^+$ scavenging activity of these compounds. $ABTS^+$ scavenging activity of compounds **10** and **12** significantly maximized concurrent the activity of compound **11** minimized, compared to their original compounds. Based on IC_{50} values, $ABTS^+$ scavenging activity of compounds **10** and **12** augmented by about 3.3 and 134.21 times, respectively compared to each corresponding original compound (**7** and **9**, respectively). On contrary, $ABTS^+$ scavenging activity of compound **11** decreased by about 4.6 times compared to original compound **8**.

$ABTS^+$ scavenging activity of compound **13** that contained cellulose molecule significant reduced than the compound **6** as IC_{50} value; 6.603 and 0.825 µg/ml, respectively. Acetylation compound **13** that produced compound **14** increased its $ABTS^+$ scavenging activity significantly by about 45.03% than the original compound (**13**) as IC_{50} value; and 6.603 and 4.553 µg/ml, respectively.

At the end, compounds from Compound **6** to Compound **14** recorded $ABTS^+$ scavenging activity more than L- ascorbic acid or Trolox, except compound **9**. Compared to compound **6**, adding disaccharide (maltose) molecules in compound **9** reduced $ABTS^+$ scavenging activity meanwhile acetylation the compound elevated $ABTS^+$ scavenging activity. Compound **10** recorded the highest $ABTS^+$ scavenging activity as the lowest

LC_{50} (0.225 µg/ml). Compound **10** IC_{50} was lower than IC_{50} of L-ascorbic acid by about 275 times, Trolox (56.09 times), and compound **6** (3.66 times).

3.5.2. Fe^{3+} ion reductive capability

Ferricyanide's oxidized Fe^{3+} form can be reduced to the reduced form (Fe^{2+}) by antioxidants and reductants. Because of this, the yellow hue of the Fe^{3+} form shifts to different green and blue Fe^{2+} hues according on the antioxidant samples' reduction power [26]. Synthetic compounds from Compound **6** to Compound **14** had a weak Fe^{3+}– Fe^{2+} transformation capability, compared to the capacity of L-ascorbic acid and Trolox ($p < 0.05$), except compound **9**. Compound **9** recorded had a high Fe^{3+}–Fe^{2+} transformation capability was equal to Trolox, where IC_{50} of both was equal (120.45 and 120.62 µg/mg, respectively). It is worth mentioning that acetylation compounds **7** and **8** that produced compounds **11** and **12** dramatically maximized their Fe^{3+}– Fe^{2+} transformation capability. According to IC_{50}, Fe^{3+}– Fe^{2+} transformation activity of two compounds was highest than their original compounds **7** and **8** as well as compound **6**. On contrast, acetylation compound **10** that produced compound **12** reduced its activity from 120.45 µg/ml to 230.93 µg/ml) (Table 1).

3.6. Assessment of *in vitro* anticancer properties

Compound **6** (the starter compound) has cytotoxicity effect against two cancer cell lines; colon carcinoma cell lines (HCT-116) and breast carcinoma cell lines (MCF-7) with IC_{50}, 122.86 and 218.47 µg/ml, respectively. Compared to Cisplatin, reference drug, cytotoxic effect of compound **6** was moderate, particularly against MCF-7 cells (Fig. 3 and Table 2).

All compounds that are produced from compound **6** have cytotoxic effect against HCT-116 more than MCF-7 cells according to IC_{50} values.

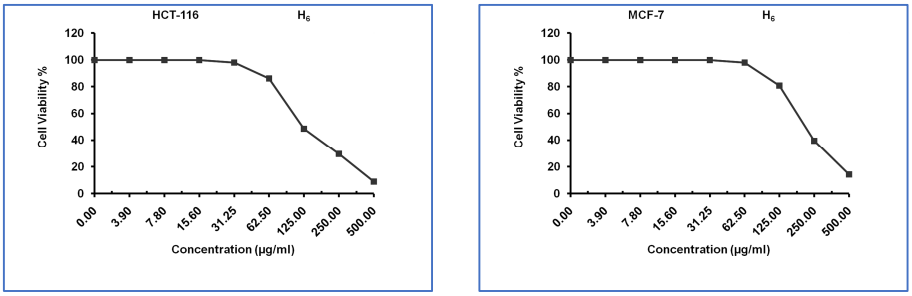

Figure 3: Cytotoxic effect of compound 6 (the starter compound) against HCT-116 and MCF-7cells.

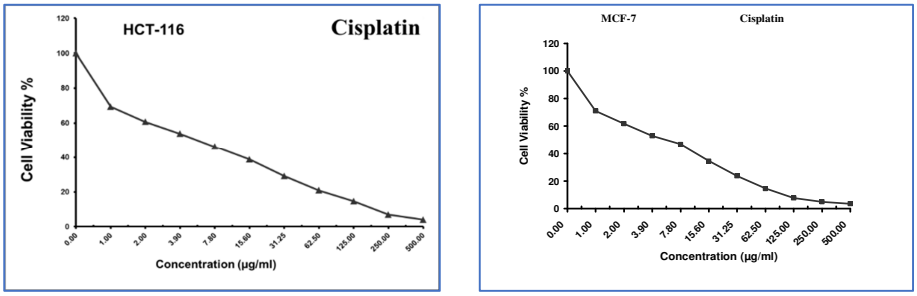

Figure 4: Cytotoxic effect of Cispaltin, reference drug, against HCT-116 and MCF-7 cells.

Adding sugars; mannose, xylose, and maltose significantly elevated the cytotoxicity of compound **6** against both cell lines. Adding mannose that produced compound **7** significantly maximized cytotoxic effect in dependent manner. HCT-116 and MCF-7 cells viability significantly reduced by compound **7** concentration was increased (viable cells accounted from 90.69 to 3.26% by concentration 3.9 to 500 µg/ml for HCT-116 cells and 98.04 to 14.29% at concentration 62.5 to 500 µg/ml, respectively) (Fig. 4). The IC_{50} value of compound **7** was lower than that of compound 6; 29.90 and 122.86 µg/ml for HCT-116 and 50.45 and 218.47 µg/ml for MCF-7 cells. Based on the IC_{50} values, adding mannose increased the cytotoxicity of compound **7** about 4.11 times against HCT-116 and 4.33 times against MCF-7 cells.

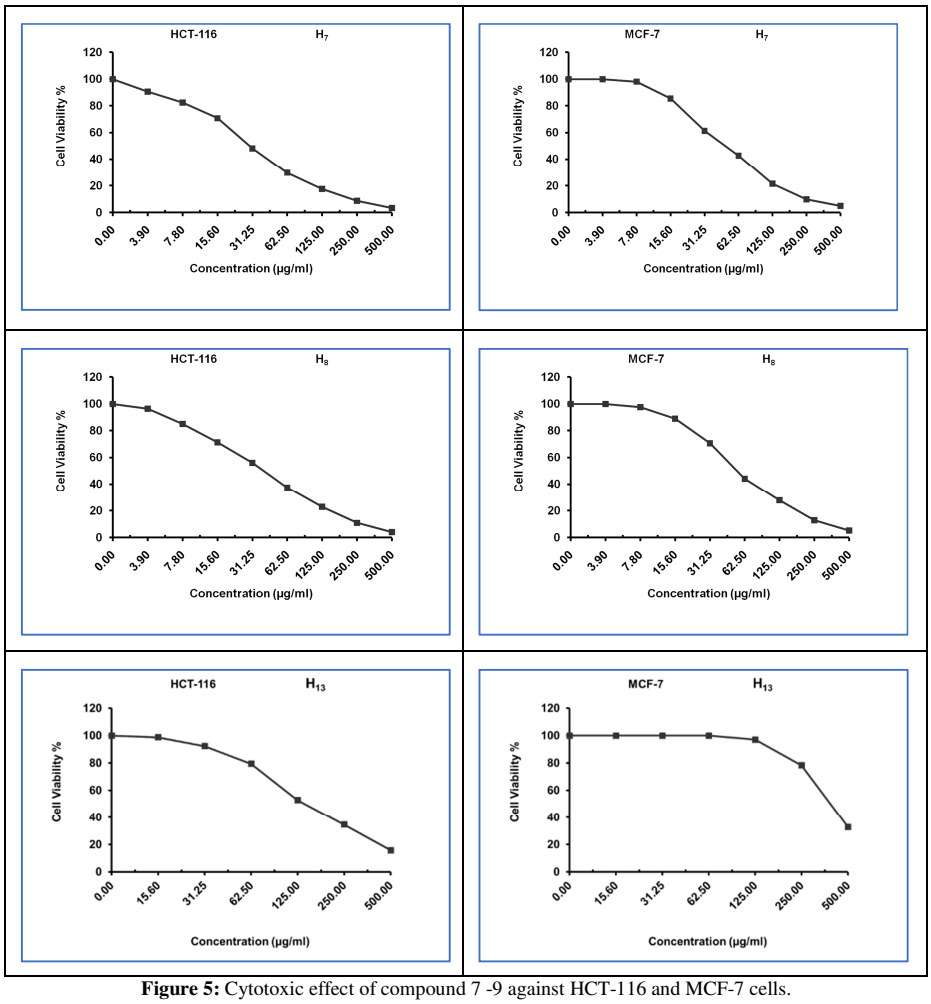

Figure 5: Cytotoxic effect of compound 7 -9 against HCT-116 and MCF-7 cells.

Compound **8** (that contains xylose) recorded cytotoxicity effect higher than compound **6** against both cancer cells. Compound **8** depleted the HCT-116 and MCF-7 proliferation and reduced cells viability significantly from 96.43% at 3.90 µg/ml to 4.07% at 500 µg/ml for HCT-116, and 100% at 3.9 µg/ml to 5.27% at 500 µg/ml for MCF-7 (Fig. 5 and Table 2). The IC_{50} value of compound **8** was lower than that of compound **6**; 41.4 and 122.86 µg/ml for HCT-116 and 55.68 and 218.47 µg/ml for MCF-7 cells. Based on the IC_{50} values, adding xylose increased the cytotoxicity of compound **8** about 3.0 times against HCT-116 and 4 times against MCF-7 cells. According to IC_{50} value, compound **8** is more effective against MCF-7 than HCT-116 cells.

Also, adding maltose elevated the cytotoxicity effect of compound **9** compared to compound **6**. The count of viable cells that treated with compound **9** was reduced from 100% to 5.97% for HCT-116 and 100% to 7.62% for MCF-7 at concentrations 3.9 to 500 µg/ml, respectively. Therefore, IC_{50} of compound **9** was lower than that of IC_{50}; 57.13 and 122.86 µg/ml for HCT-116, and 87.12 and 218.47 µg/ml for MCF-7, respectively.

Acetylation compounds **7**, **8**, and **9** that produced compounds **10**, **11**, and **12** significantly reduced their cytotoxic effect against both cell lines than corresponding original compounds. Although, the anti-proliferative effect of the acetylated compounds was best than compound **2**. According to IC_{50} values, acetylated compound **10**, **11**, and **12** (83.06, 53.98, and 60.60 µg/ml) showed cytotoxic effect lower than their original compounds (29.90, 41.48, and 60.60, respectively) **Fig. 6**.

Table 2: Cytotoxic effect of compounds against HCT-116 and MCF-7 cells, compared to Cisplatin as IC_{50}.

Compounds	Anticancer effect of compounds IC_{50} (µg/ml)	
	Colon carcinoma cells (HCT-116)	Breast carcinoma cells (MCF-7)
Compound 6	122.86 ± 3.17	218.47 ± 5.93
Compound 7	29.90 ± 0.92	50.45 ± 3.06
Compound 8	41.48 ± 1.23	55.68 ± 3.18
Compound 9	57.13 ± 1.78	87.12 ± 4.65
Compound 10	83.06 ± 2.95	216.39 ± 8.19
Compound 11	53.98 ± 1.86	69.03 ± 3.68
Compound 12	60.60 ± 2.09	93.14 ± 4.17
Compound 13	144.04 ± 6.07	405.85 ± 16.38
Compound 14	98.12± 4.31	206.18 ± 6.59
Cisplatin (reference drug)	5.38 ±0.44	5.73 ± 0.59

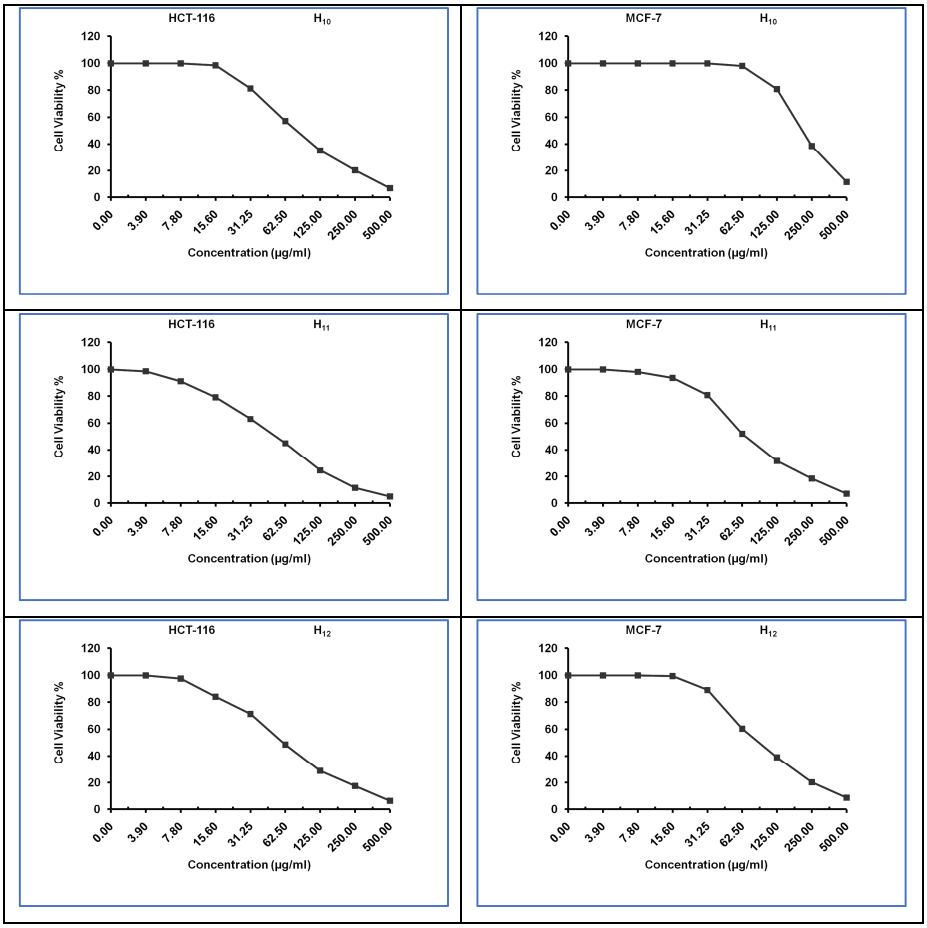

Figure 6: Cytotoxic effect of acetylated compound 10, 11, and 12 against HCT-116 and MCF-7 cells.

On the contrary, adding cellulose in compound **13** showed anti-proliferative effects lesser than that recorded by compound **6** against both cell lines. Compound **13** inhibited HCT-116 cell growth by 1.2% at concentration 15.6 µg/ml that increased to 84.24% at 500 µg/ml compared to compound 6 (1.84 to 91.09% by concentrations 31.55 to 500 µg/ml). Also, IC_{50} of compound **13** suppressed MCF-7 cells growth by 2.87% at 25 µg/ml and 67.09% at 500 µg/ml, compared to (1.96% at 62.5 µg/ml to 85.71% at 500 µg/ml).

In addition, IC_{50} of compound **13** was higher than that of compound **1**; 144.04 and 122.86 µg/ml for HCT-116. However, IC_{50} of compound **13** was lesser than of compound **6** against MCF-7; 405.85.18 and 218.47 µg/ml.

Compound **14** exhibited the opposite trend, where acetylation compound **13** that produced compound **14** increased its cytotoxic effect against both cell lines to be higher than original compound (**13**) and compound **6**. Based on the IC_{50} value, compound **14** has cytotoxic effect higher than compound **13** by about 31.88% for HCT-116 and 49.20% for MCF-7 cell as well as compound **2** (20.14% for HCM-116 cells and 5.63% for MCF-7 cells) (**Fig. 7**).

From the explained data we can conclude that, from three added sugars, mannose exhibited the best effect. However, the activity of compound **7** was still lower than that of Cisplatin according IC_{50}. Adding short chain sugars as mannose, xylose and maltose was more active than adding long chain sugars as cellulose. Acetylation compounds reduced their activity than original compounds (non-acetylated compounds). Finally, all compounds have anti-proliferative effect lower than Cisplatin, the reference drug).

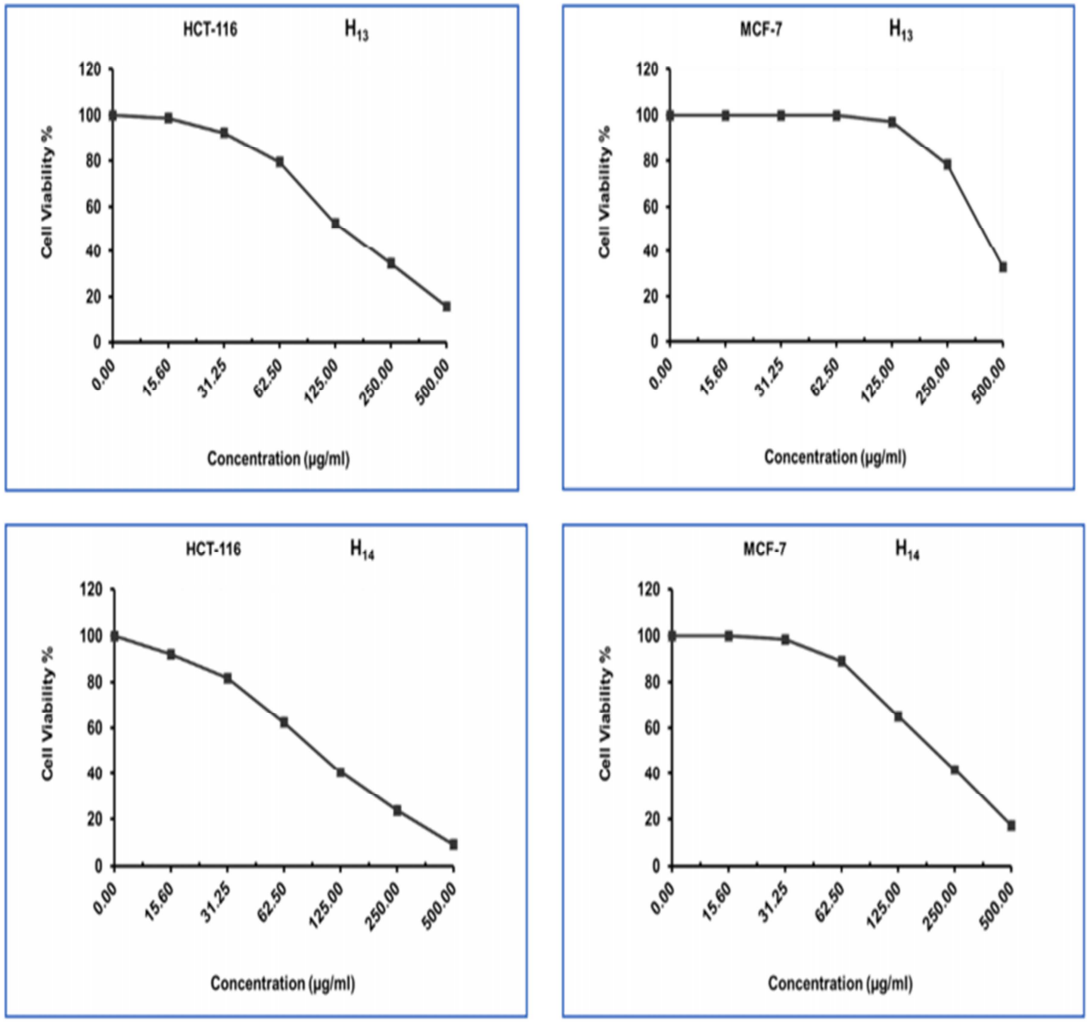

Figure 7: Cytotoxic effect of acetylated compound 13 and 14 against HCT-116 and MCF-7 cells.

4. Discussion

In chemistry, benzmidazole is an aromatic heterocycle, classified as a diazole, and has non-adjacent nitrogen atoms in meta-substitution. Many natural products, especially alkaloids, contain the imidazole ring. These benzimidazoles share the 1,3-C_3N_2 ring but feature varied substituents. This ring system is present in important biological building blocks, such as histidine and the related hormone histidine [27]. Many drugs contain a benzimidazole ring, such as certain antifungal drugs, the nitroimidazole series of antibiotics, and the sedative midazolam. Imidazole substituents are found in many pharmaceuticals. Numerous medications, including certain antifungals, antibiotics of the nitroimidazole class, and the sedative midazolam, have a benzimidazole ring. A wide range of pharmaceutical products contain imidazole substituents. Numerous fungicides, as well as antifungal, antiprotozoal, and antihypertensive drugs, contain synthetic benzimidazoles. Theophylline, a chemical included in coffee beans and tea leaves that stimulates the central nervous system, includes imidazole. It can be found in the anticancer drug mercaptopurine, which interferes with DNA functions to treat leukemia [28]. Imidazole, a five-membered heterocycle, is highly polar due to the presence of two nitrogen atoms. Imidazole can act as a hydrogen bond donor if it is not substituted at N1 and is also capable of coordinating metals. In addition to hydrogen bonding and coordination, imidazole can participate in van der Waals interactions, π–π stacking, cation–π interactions, and other interactions.

Compounds containing an imidazole ring display a wide range of pharmacological activities including anticancer [29], antibacterial [30], antiviral [31], antiepileptic [32], antitubercular [33], and antifungal activities [30]. A range of anticancer drugs, such as dacarbazine, bendamustine hydrochloride, fludarabine phosphate, nilotinib, and ponatinib, contain imidazole and fused imidazole as structural components.

Imidazoles have many anticancer mechanisms as tubulin polymerization inhibitors, kinase inhibitors, DNA intercalators inhibitor, topoisomerase inhibitors, inhibitors of minichromosomal maintenance proteins, poly (ADP-Ribose) polymerase (PARP) inhibitors, histone deacetylase (HDAC) inhibitors, lysine-specific demethylase 1 (KDM1A) inhibitors, p53-murine double minute 2 (MDM2) inhibitors, bromodomain and extraterminal (BET) protein inhibitors, WD repeat domain 5 (WDR5) inhibitors, signal transducer and activator of transcription 3 (STAT3) inhibitors, indoleamine-2,3-dioxygenase (IDO)/tryptophan 2,3-dioxygenase (TDO) signaling inhibitors, aromatase inhibitors, inhibition of aldehyde dehydrogenase, galectin-1 inhibitors, lipoxygenase inhibitors, estrogen receptor-α (ER-α) inhibitors, ABCB1 inhibitors and heat shock protein (HSP) inhibitors [27].

Alkaline and bleaching treatments had the anticipated effect of increasing the cellulose content in cotton stalk composition. The main substance that gives plant cell walls their structural integrity and stiffness is cellulose. Glucose units are organized in a linear polymer framework to form cellulose, an abundant organic compound. In general, 25–50% cellulose, 25–40% hemicellulose, and 10–20% lignin are found in non-woody biomass [34]. Alkali treatment causes hemicelluloses, lignin, and silica to dissolve, swell cellulose, and decrease cellulose crystallinity, all of which disrupt the cell wall [35]. The -CH rocking vibrations typical of the cellulose backbone and the glycosidic bonds between glucose units were shown by the band at 875 cm^{-1}. According to reports, the anomeric vibration of -glucosides (C-H vibration of cellulose) is represented by the band at 892-896 cm^{-1}. The bands between 2800 and 2900 cm^{-1} are hypothesised to be caused by the crystalline structure of cellulose [36]. The wide absorbance band in the 3300–3500 cm^{-1} range of the NCC spectra was ascribed to the stretching of single bond OH groups. The shrinking of this band from the NCC benzoimidazole and acetalyated NCC benzoimidazole spectra indicates that the substituted functional groups of the cellulose chains affected varying amounts of free single bond OH groups. NCC cotton stalk, maize stalk, and rice straw were found to be between 71.5-86.6 nm, 22.5-46.2 nm, and 46.4-63.2 nm, respectively, while NCC bagasse particles ranged from 19.1-45.4 nm [37].

Many substitutions processes were performed on imidazole, some of them increased its activity and others reduced it. In the present study, all added sugars significantly increased imdazole anticancer activity. These results were agreed with Tuncbilek et al. (2018) who synthesized β-D-ribofuranosyl-purine derivatives that increased the anticancer activity against Huh7, HCT116, and MCF-7 cell lines [38]. The authors suggested that substitution of imidazole ring on monosaccharaides and disaccharides were increased the biological activity may be due to the increase of hydroxyl groups. Unfortunately, the acetylated derivatives compounds were have less activity than their original compounds depend on decreasing the free hydroxyl groups.

On contrast, cellulose imidazole derivative showed antioxidant and anticancer activity less than all substituted sugars imidazole derivatives, these may be due to its helicstucture and high molecular.

On the other hand the acetylated cellulose imidazole increased as antioxidant and anticancer activity. The authors suggested that the solubility of cellulose weight imidazole was increase which reflected on its biological activities.

5. Conclusion

In conclusion, the anticancer screening suggests that all the newly synthesized compounds showed good to very good activity. Hence the fact that the compounds prepared in this study are chemically unrelated to the current medication, suggests that further work with similar analogues is clearly warranted. In the present study, all added sugars; mannose, xylose, and maltose significantly increased 2-methyl thio-1H-benzimidazol anticancer activity against HCT-116 and MCF-7, except cellulose. Mannose substitution (Compound **7**) recorded the highest activity against both cancer cell lines, compared to imidazole compound. The acetylation of derivatives compounds did not increase their anticancer activities. It is evident from the study that newly synthesized compounds can be incorporated in further advanced medical studies as anticancer material.

Funding

There was no external support for this study

Acknowledgment

The authors are pleased to present their sincere gratitude to the National Research Center, Cairo, Egypt and Faculty of Science, Menoufia University for continuous support for completing the presented research.

Conflicts of Interest

The authors declare no conflict of interest.

References

[1] World Health Organization (WHO), 2024. Breast cancer https://www.who.int/news-room/fact-sheets/detail/breast-cancer. 11 March 2024.

[2] World Health Organization (WHO), 2023. Colorectal cancer https://www.who.int/news-room/fact-sheets/detail/colorectal-cancer. 11 July 2023.

[3] Chrysanthos, M., 2020. Production of Sustainable and Biodegradable Polymers from Agricultural Waste, Polymers. 12(5), 1127, https://doi.org/10.3390/polym12051127.

[4] Magdy, Z., Mahmoud, K., Reem, K. F., Nermen, M., Samya, E., 2021. Assessment of green biodiesel production based on Egyptian waste cooking oil using different porous membranes, Egyptian Journal of Chemistry. 64(8), 4401-4415.

[5] Abdel-Rahman, A. A. H., Nassar, I. F., El-Kattan, I. M. H., Aly, A. A., Behalo M. S and Abdelwahed, N. A. M. (2013) Synthesis and antimicrobial evaluation of thioglucosides and acyclic Cnucleosides of 2-methylbenzimidazole Der Pharma Chemica, 5(1):210-217.

[6] Göker, A. H., Ayhan-Kilcigil, G., Tunçbilek, M., Kuş, C., Ertan, R., Kendi, E., Özbey, S., Fort, M., Garcia, C., Farré, A. J., 1999. Synthesis and antihistaminic H1 activity of 1,2,5(6)-trisubstituted benzimidazoles, Heterocycles. 11(51), 2561-2573.

[7] Podunavac, K., Sanja, O., Ćetković, G. S., Leovac, V.M., Markov, S., Rogan, J., 2001. Physico-chemical characterization and antibacterial-activity of copper(II), zinc(II) and nickel(II) complexes with 2-methylbenzimidazole, Acta periodica technologica. (32), 145-150.

[8] Laura, G., Marinella, R., Claudio, C., 1999. Synthesis and antiviral activity of some N-benzenesulphonylbenzimidazoles, Bioorganic & Medicinal Chemistry Letters. 17(9), 2525-2530.

[9] Vieira, R.G.P., Rodrigues, F.G., Assunção, R.M.N., Meireles, C.S., Vieira, J.G., Oliveira, G.S., 2007. Synthesis and characterization of methylcellulose from sugar cane bagasse cellulose, Carbohydrate Polymers. 67(2), 182–189. https://doi.org/10.1016/j.carbpol.2006.05.007.

[10] Naomi, R., Bt Hj Idrus, R., Fauzi, M.B., 2020. Plant- vs. Bacterial-Derived Cellulose for Wound Healing: A Review, Int. J. Environ. Res. Public Health. 17(18), 6803. https://doi.org/10.3390%2Fijerph17186803.

[11] Zahid, H.C., Humayun, P., Abdul R., Andrea, S., Claudiu, T.S., 2008. Antibacterial Co(II), Cu(II), Ni(II) and Zn(II) Complexes of Thiadiazole Derived Furanyl, Thiophenyl and Pyrrolyl Schiff Bases, Enzyme Inhibition and Medicinal Chemistry. 16(2), 117-122.

[12] Ragab, T.I. M., Shalaby, S. G., El Awdan, A. S., Refaat, A., Helmy, W.A., 2018. New applied pharmacological approach/trend on utilization of agro-industrial wastes, Environmental Science and Pollution Research. 25, 26446–26460.

[13] Shuyu, L., Tao, M., Xinna, H., Jing, Z., Xiaojun, L., Yi, S., Xiaosong, H., 2021. Facile extraction and characterization of cellulose nanocrystals from agricultural waste sugarcane straw, Science of food and Agriculture. 102(1), 312-321. https://doi.org/10.1002/jsfa.11360.

[14] Paralikar, K.M., Aravindanath, S., 1988. Crystallization of cellulose, Applied Polymer Science. 35(8), 2085–2089. https://doi.org/10.1002/app.1988.070350809.

[15] Ragab, T.I. M., Fouda, A. A., Azab, M. M., Wasfy, A.A.F., Jamil, T. S., 2024. Water Desalination Graphene Oxide/Ca Ro Membranes Manufactured From Date Palm Fibers' Microcrystalline Cellulose, Egypt. J. Chem. 67 (7), 301 - 318.

[16] Helmy, W.A., Ragab, T.I.M., Salama, B.M., Basha, M., Shamma, R., Abd El-Rahman, S.S., Shawky, H., 2023. Novel naringin tablet

formulations of agro-resides based nano/micro crystalline cellulose with neuroprotective and Alzheimer ameliorative potentials, International Journal of Biological Macromolecules. 231, 123060.

[17] Esawy, M.A., Tamer, I.M.R., Basha, M., Emam, M., 2019. Evaluated bioactive component extracted from Punica granatum peel and its Ag NPs forms as mouthwash against dental plaque, Biocatalysis and Agricultural Biotechnology. 18, 101073

[18] Ragab, T.I.M., Nada, A.A., Ali, E.A., Soliman, A.A.F., Emam, M., El Raey, M.A., 2019. Soft hydrogel based on modified chitosan containing P. granatum peel extract and its nano-forms: Multiparticulate study on chronic wounds treatment, International journal of biological macromolecules. 135, 407-421, 2019.

[19] Yamaguchi, F., Saito, M., Ariga, T., Yoshimura, Y., Nakazawa, H., 2000. Free radical scavenging activity and antiulcer activity of garcinol from Garcinia indica fruit rind, J. Agric. Food Chem. 48, 2320–2325. https:// doi. org/ 10. 1021/ jf990 908c

[20] Miller, N.J., Rice-Evans, C.A., 1997. The relative contributions of ascorbic acid and phenolic antioxidants to the total antioxidant activity of orange and apple fruit juices and blackcurrant drink. Food Chem. 60, 331–337. https:// doi. org/ 10. 1016/ S0308- 8146(96) 00339-1

[21] Arnao, M.B., Cano, A., Acosta, M., 2001. The hydrophilic and lipophilic Contribution to total antioxidant activity. Food Chem. 73, 239–244, https:// doi. org/ 10. 1016/ S0308- 8146(00) 00324-1

[22] Rani, N., Sharma, A., Gupta, G.K., Singh, R., 2013. Imidazoles as potential antifungal agents: A review, Mini Rev. Med. Chem. 13, 1626–1655.

[23] Mosmann, T., 1963. Rapid colorimetric assay for cellular growth and survival: application to proliferation and cytotoxicity assays, J. Immunol. Methods. 65, 55–63. https:// doi. org/ 10. 1016/ 0022-1759(83) 90303-4

[24] Gomha, S.M., Riyadh, S.M., Mahmmoud, E.A., Elaasser, M.M., 2015. Synthesis and Anticancer Activities of Thiazoles, 1,3-Thiazines, and Thiazolidine Using Chitosan-Grafted-Poly(vinylpyridine) as Basic Catalyst, Heterocycles. 91(6), 1227-1243, https://doi.org/10.1007/s11356-018-2631-9.

[25] Ibrahim, F.N., Dina, S.E., Hanem, M., Wael, A.E., 2019. Design, Synthesis, and Anticancer Activity of New Oxadiazolyl-Linked and Thiazolyl-Linked Benzimidazole Arylidines, Thioglycoside, and Acyclic Analogs, Heterocyclic Chem. 56, 1086-1099.

[26] Oyaizo, M., 1986. Studies on products of browning reaction: antioxidative activities of products of browning reaction prepared from glucosamine, Jpn. J. Nutr. Diet. 44, 307–315. https:// doi. org/ 10. 5264/eiyog akuza shi. 44. 307.

[27] Sharma, P., LaRosa, C., Antwi, J., Govindarajan, R., Werbovetz, K.A., 2021. Imidazoles as Potential Anticancer Agents: An Update on Recent Studies, Molecules. 26, 4213. https://doi.org/ 10.3390/molecules26144213.

[28] Tolomeu, H.V., Fraga, C.A.M., 2023. Imidazole: Synthesis, Functionalization and Physicochemical Properties of a Privileged Structure in Medicinal Chemistry, Molecules. 28, 838. https://doi.org/10.3390/molecules28020838

[29] Ali, I., Lone, M.N., Aboul-Enein, H.Y., 2017**.** Imidazoles as potential anticancer agents, Med. Chem. Commun. 8, 1742–1773.

[30] Rani, N., Sharma, A., Singh, R., 2013. Imidazoles as promising scaffolds for antibacterial activity: A review, Mini Rev. Med. Chem. 13, 1812–1835.

[31] Zhan, P., Liu, X., Zhu, J., Fang, Z., Li, Z., Pannecouque, C., de Clercq, E., 2009 Synthesis and biological evaluation of imidazole thioacetanilides as novel non-nucleoside HIV-1 reverse transcriptase inhibitors, Bioorg. Med. Chem. 17, 5775–5778.

[32] Mishra, R., Ganguly, S., 2012**.** Imidazole as an anti-epileptic: An overview, Med. Chem. Res. 21, 3929–3939.

[33] Fan, Y.L., Jin, X.H., Huang, Z.P., Yu, H.F., Zeng, Z.G., Gao, T., Feng, L.S., 2018**.** Recent advances of imidazole-containing derivatives as anti-tubercular agents, Eur. J. Med. Chem. 150, 347–365.

[34] Langsdorf, A., Volkmar, M., Holtmann, D., Ulber, R., 2021. Material utilization of green waste: a review on potential valorization methods, Bioresour. Bioprocess. 8, 1–26.

[35] Brodeur, G., Yau, E., Badal, K., Collier, J., Ramachandran, K.B., Ramakrishnan, S., 2011. Chemical and Physicochemical Pretreatment of Lignocellulosic Biomass: A Review, Enzyme Research Volume. Article ID787532, 17pages, doi:10.4061/2011/787532.

[36] Salim, R.M., Asik, J., Sarjadi, M.S., 2021. Chemical functional groups of extractives, cellulose and lignin extracted from native Leucaena leucocephala bark. Wood Science and Technology. 55, 295-313, https://doi.org/10.1007/s00226-020-01258-2.

[37] Arowona, M.T., Olatunji, G.A., Saliu, O.D., Adeniyi, O.R., Atolani, O., Adisa, M.J., 2019. Thermally Stable Rice Husk Microcrystalline Cellulose as Adsorbent in PTLC Plates, JOTCSA. 5(3), 1177-1184, DOI: http://dx.doi.org/10.18596/jotcsa.327665.

[38] Tuncbilek, M., Kucukdumlu, A., Guven, E.B., Altiparmak, D., Cetin-Atalay, R., 2018. Synthesis of novel 6-substituted amino-9-(_-Dribofuranosyl) purine analogs and their bioactivities on human epithelial cancer cells, Bioorg. Med. Chem. Lett. 28, 235–239.